Cell, Vol. 86, 115–121, July 12, 1996, Copyright ©1996 by Cell Press

The COP9 Complex, a Novel Multisubunit Nuclear Regulator Involved in Light Control of a Plant Developmental Switch

Daniel A. Chamovitz,*‡ Ning Wei,* Mark T. Osterlund,* Albrecht G. von Arnim,*§ Jeffrey M. Staub,* Minami Matsui,† and Xing-Wang Deng*
*Department of Biology
Yale University
New Haven, Connecticut 06520-8104
†Laboratory of Photoperception
and Signal Transduction
RIKEN
Saitama 351-01
Japan

Summary

Arabidopsis COP9 is a component of a large protein complex that is essential for the light control of a developmental switch and whose conformation or size is modulated by light. The complex is acidic, binds heparin, and is localized within the nucleus. Biochemical purification of the complex to near homogeneity revealed that it contains 12 distinct subunits. One of the other subunits is COP11, mutations in which result in a phenotype identical to *cop9* mutants. The COP9 complex may act to regulate the nuclear abundance of COP1, an established repressor of photomorphogenic development. During the biogenesis of the COP9 complex, a certain degree of prior subunit association is a prerequisite for proper nuclear translocation. Since both COP9 and COP11 have closely related human counterparts, the COP9 complex probably represents a conserved developmental regulator in higher eukaryotes.

Introduction

As plants are sessile organisms and must adjust to the ambient conditions where they are located, they have developed highly sophisticated photosensory and transductory mechanisms to allow the modulation of development in response to light quantity, quality, and direction, thus maximizing their chance of survival. The effect of light on plants is most evident in seedling development (McNellis and Deng, 1995). Seedlings of dicotyledonous angiosperms develop according to one of two distinct developmental pathways depending on the ambient light conditions. Dark-grown seedlings undergo skotomorphogenesis, while light-grown seedlings undergo photomorphogenesis. Accumulated data suggest that multiple photoreceptors, including phytochrome A, phytochrome B, and CRY1, are responsible for sensing specific wavelengths of light signals to modulate gene expression and consequently the pattern of seedling development (Quail et al., 1995; Ahmad and Cashmore, 1993). Several potential signaling components downstream of phytochrome, such as trimeric G protein(s), cGMP, and calcium/calmodulin have been revealed (Bowler and Chua, 1994).

Genetic screens employed to identify the key components involved in the light control of seedling developmental pattern have converged recently on ten Arabidopsis pleiotropic *COP/DET/FUS* loci (Castle and Meinke, 1994; Miséra et al., 1994; Kwok et al., 1996). Recessive mutations in any of these loci result in pleiotropic photomorphogenic seedling development in darkness, mimicking light-grown plants both morphologically and at the level of gene expression. Four of the genes, *COP1* (Deng et al., 1992), *COP9* (Wei et al., 1994b), *COP11/FUS6* (Castle and Meinke, 1994), and *DET1* (Pepper et al., 1994), have been cloned and characterized. Since all mutations isolated are loss-of-function in nature, it was proposed that these loci encode negative regulators that act to repress photomorphogenic seedling development in the dark. Both COP1 and DET1 appear to function within the nucleus, although the nuclear localization of COP1 is subject to light modulation (Pepper et al., 1994; von Arnim and Deng, 1994).

The phenotypic similarity among the pleiotropic *cop/det/fus* mutants implies that some of them may encode subunits of multiprotein complexes. Indeed, in initial biochemical fractionation studies of Arabidopsis, COP9, a small hydrophilic 22 kDa protein, was found to exist only in a large protein complex whose conformation or size is modulated by light (Wei et al., 1994b). The fact that COP9 protein failed to accumulate in both *cop8* and *cop11* mutants further suggested that COP8 and COP11 are either additional components of this complex or are necessary for its formation and stability (Wei et al., 1994b). As a major step in our effort to understand the role of the COP9 complex and its functional relationship to other pleiotropic *COP/DET/FUS* loci in light control of plant development, we report here the biochemical purification and characterization of this complex, its subcellular localization, and its functional relationship with other pleiotropic *COP/DET/FUS* gene products.

Results

Biochemical Purification of the COP9 Complex

In our evaluation of the proper tissue type for the biochemical purification of the COP9 complex, we noted that young Arabidopsis flower buds had the highest cellular content of COP9 (data not shown). Owing to the practical limitation of Arabidopsis flower tissue, heads of Brassica oleracea L. (cauliflower), a member of the same Brassica family as Arabidopsis, which are comprised primarily of young flower tissue and are abundantly available, were chosen for the complex purification. Western blot analysis of cauliflower head extracts revealed a protein of identical mobility to Arabidopsis COP9, which was present in highest amounts among all tissue types examined (data not shown). Further size fractionation of the soluble protein extracts indicated

‡Present address: Department of Botany, Tel Aviv University, Ramat Aviv 69978, Israel.
§Present address: Department of Botany, University of Tennessee, Knoxville, Tennessee, 37996.

Table 1. Outline of Purification Procedure and Fold Purification for COP9 and COP11

Step	Fold Purification COP9	COP11
Total cell homogenate	1	1
Q Sepharose Fast Flow anion ion exchange	5	6
Q Sepharose HP anion ion exchange	85	90
Heparin affinity column	162	172
Mono Q anion ion exchange	194	206
Superose 6 HR gel filtration	426	437

Only the major steps are shown. The full purification procedure is detailed in Experimental Procedures. Fold purification was determined by quantitative Western blot analysis of COP9 and COP11 from each step (data not shown) with densitometry scanning of the COP9- and COP11-corresponding bands in the Western blots. Typical yields of purified complex were about 0.5% to 1%.

Table 2. Summary of the COP9 Complex Components

Protein Bands[a]	Peptice Profile[b]	Estimated Molar Ratio[c] (I)	(II)	Subunit Designation
p90	Unique	?	?	12
p71	Unique	ND	1.3	11
p56	Unique	ND	1.2	10
p52	Similar to p50	0.4	ND	9 (COP11)
p50	Similar to p52	0.6	ND	9 (COP11)
p46	Unique	1.0	ND	8
p43	Unique	0.9	ND	7
p42	Unique	1.1	1.4	6
p41	Unique	0.7	ND	5
p39	ND	<0.1	ND	No
p36	ND	<0.1	ND	No
p34	Unique	1.1	ND	4
p27	Unique	ND	1.1	3
p25	Unique	0.9	ND	2
p22	Unique	1.0	1.0	1 (COP9)

[a]The 15 protein bands listed are those that exhibited strong silver staining following SDS–PAGE (see Figure 1C). Both p52 and p50 represent the COP11 subunit (see text).

[b]All excised protein bands were subjected to total peptide profile analysis after proteinase digestion, and in most cases two or more peptides were sequenced. Except for p52 and p50, no obvious similarities were found among other protein bands analyzed.

[c]The molar ratios were determined using two different methods, and in both cases the COP9 was set as 1 relative unit. In (I), the protein bands were excised from the SDS–polyacrylamide gel and subjected to proteinase digestion, and resulting peptides were fractionated. The molar amount of a given peptide was calculated according to its spectrometric reading (see Experimental Procedures) and its exact amino acid sequences. In (II), the protein bands were excised from the SDS–polyacrylamide gel and subjected to total amino acid quantitation. The ratios were then calculated based on the total amino acid quantity and their respective molecular masses. Both p36 and p39 were present in much smaller molar amounts and thus unlikely to be subunits of the complex. The molar amount for p90 is not available owing to difficulty in determining peptide sequence. However, the peak sizes of the peptide profile of p90 were similar to the other major protein bands. ND, not determined.

that the cauliflower COP9 elution profile is identical to that of Arabidopsis, with a single peak around 560 kDa and devoid of any monomeric form. Quantitative Western blot analysis indicated that COP9 in total cauliflower head protein extracts represents approximately 0.01% of total soluble protein. Assuming one COP9 subunit (22 kDa) per complex (560 kDa), only about 400-fold enrichment is necessary to purify the COP9 complex completely.

By monitoring the presence of COP9 through Western blot assay, the COP9 complex was purified from cauliflower head extracts through an empirically determined purification scheme (see Table 1 and Experimental Procedures). Several properties of the complex are evident from the purification procedure. The complex is acidic, binding a quaternary ammonium (Q) anion exchange column at pH 5.7. The complex has affinity for heparin, a highly sulfated glycosaminoglycan with the ability to bind nucleic acid–binding proteins. The complex elutes in the final step as a single gel filtration peak of 560 kDa (Figure 1A), indicating that the purified product has retained its original dimensions.

To examine the physical homogeneity and dimensions of the purified COP9 complex, the COP9 complex containing fraction (peak II in Figure 1A) was subjected to negative staining with uranyl acetate and examined by transmission electron microscopy. As illustrated in Figure 1B, the purified COP9 complexes appear as uniform spherical particles of approximately 12 nm diameter, consistent with the predicted molecular mass of about 560 kDa.

Portions of the gel filtration fractions (Figure 1A) were separated by SDS–polyacrylamide gel electrophoresis (SDS–PAGE) and visualized by silver staining. As shown in Figure 1C, a total of 15 major stained bands were found in the COP9-containing fraction corresponding to the center of the major peak (II) in the elution profile (Figure 1A) and were marked according to their apparent molecular mass. One of the proteins, p22, strongly reacts with anti-COP9 antibodies (Figure 1C). Furthermore, a 23 amino acid internal peptide (LWTRDYAGVYE AIRGFDWSQDAK) from p22 was sequenced and found to be identical to residues 86–108 of Arabidopsis COP9 in 20 of the 23 residues (Wei et al., 1994b). Thus, it definitively confirmed p22 as cauliflower COP9.

COP11 Is a Subunit of the COP9 Complex

To test whether COP11 is present in the purified COP9 complex, we probed a protein blot with the above peak II with COP11-specific antibodies. As shown in Figure 1C, the COP11 antibodies strongly react with both p52 and p50. To confirm the identity of p52 and p50 as COP11, two contiguous internal peptides from p52 and one internal peptide from p50 were sequenced and found to be 100% identical to residues 381–416 (for p52) and 401–416 (for p50) of Arabidopsis COP11 (data not shown; Castle and Meinke, 1994). Since both p22/COP9 and p52/p50/COP11 were equally enriched during each step of the purification (Table 1) and are present in similar molar ratios in the purified complex (Table 2), we conclude that COP11 is a subunit of the COP9 complex and not simply a result of serendipitous copurification with COP9. This conclusion was further confirmed by our observation that in Arabidopsis seedlings, COP11 cofractionated with COP9 in the same high molecular mass fractions and they coimmunoprecipitated together

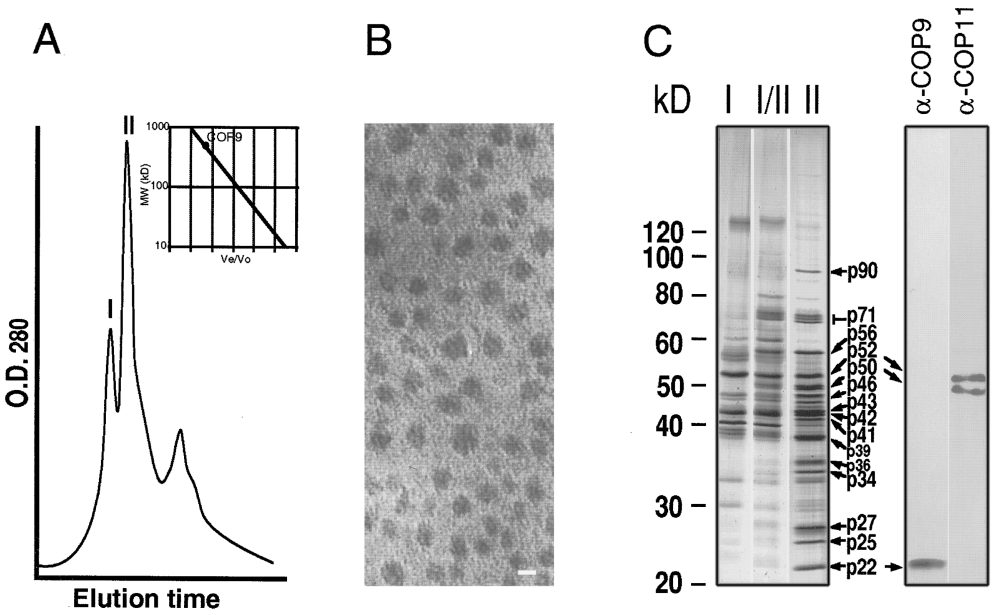

Figure 1. Purification and Characterization of the COP9 Complex from Cauliflower

(A) Final gel filtration step. Shown is the protein elution profile from the Superose 6 HR column. COP9 was found only in peak II. The calibration curve is shown in the upper right corner of the monitor trace.

(B) Electron microscopic view of the COP9 complex (peak II sample) after negative staining. The particles are approximately 12 nm diameter in size, as indicated by the scale bar (12 nm).

(C) Silver-stained proteins from the centers of peaks I and II and the valley (I/II) between them and immunoblot detection of COP9 and COP11 in peak II. p36 and p39, shown in smaller type, are most likely not components of the complex (see Table 2). The identity of COP9 and COP11 was further confirmed by amino acid sequencing. It should be noted that p71 migrates as a single protein band in some other gels.

(J. M. S. and X.-W. D., unpublished data). The fact that COP11 is a component of the COP9 complex not only clarifies our previous genetic prediction, but further confirms that we have succeeded in purifying the COP9 complex. Since p50 and p52 are present in submolar levels compared with COP9 and the other subunits (see below and Table 2) and the relative amounts of the p50 and p52 were quite variable during purification, the presence of two COP11 species is likely a consequence of the purification procedure.

The Purified COP9 Complex Contains 12 Subunits

Several lines of evidence indicate that the COP9 complex has been purified and that the major protein components copurified with COP9 are the subunits of the complex. First, the overall fold of enrichment for COP9 (Table 1) is similar to that predicted for purification of the COP9 complex, assuming one COP9 molecule per complex. Second, both COP9 and COP11 were equally enriched throughout the purification scheme (Table 1). Third, modifications of the purification scheme affected the yield, but not the composition, of the purified complex (data not shown). Fourth, the complex was purified in moderately high ionic strength (up to 0.6 M) and also is stable under 4 M urea (data not shown), conditions that do not favor nonspecific aggregation. Fifth, the uniform negatively stained particles of correct dimensions seen in the COP9 fraction are consistent with the complex being the major species.

To determine the subunit composition of the purified complex, the identity of the 15 intensely stained protein bands shown in Figure 1C and their relative molar amounts were analyzed. The identities of the protein bands in the purified complex were analyzed by their proteinase (Achromobacter protease I and trypsin)-digested peptide profiles. Two protein bands, p36 and p39, contain less than 10% of the protein found in the other bands and thus were not suitable for accurate analysis. This is consistent with our observation that these two proteins were barely detectable in the Coomassie blue–stained preparative SDS–PAGE of the purified complex used for purifying the individual proteins for peptide sequencing. It is likely that these two bands are minor contaminating proteins that are hypersensitive to silver staining and are not subunits of the COP9 complex. The peptide profiles from 11 of the other 13 protein bands were unique (Table 2). As expected, the profiles for p52 and p50, which both represent COP11, were similar. Therefore, there are likely a total of 12 distinct protein subunits in the complex.

To reveal the molar ratios of the 12 distinct subunits, the molar amounts of each protein relative to COP9 in the purified complex were analyzed by two different methods (see Table 2 and legend). Except for p90, for which we still have not obtained a peptide sequence and are thus unable to determine the molar content accurately, the relative molar amounts of the remaining protein subunits were determined (Table 2). Of the protein bands analyzed (including COP9), 10 were found in approximately equal molar amounts (ranging from 0.7 to 1.4 M when compared with COP9). The two COP11

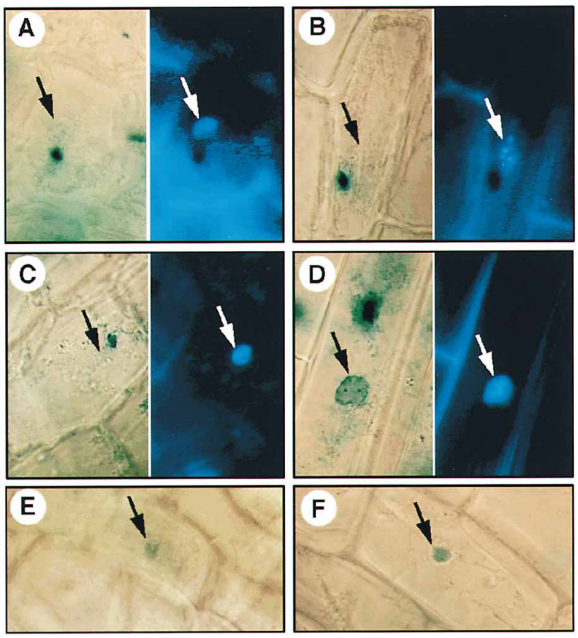

Figure 2. Absence of GUS–COP1 Nuclear Staining in Young Hypocotyl Cells of *cop9* Mutant Seedlings

GUS–COP1 subcellular staining patterns in young hypocotyl cells of *cop9* mutant seedlings grown in the light (A) and dark (B) and in wild-type seedlings grown in the light (C) and dark (D). GUS–NIa fusion proteins properly localize to the nucleus in *cop9* mutants, both in the light (E) and dark (F). DAPI staining of the nuclear position in (A)–(D) (indicated by open arrows) is shown to the right of the GUS staining of the same cells.

bands, p52 and p50, each had approximately half the molar amount of COP9. Therefore, p52 and p50 represent heterogenous forms of the same protein subunit, COP11, while the other 11 major protein components represent distinct subunits. Together, our results suggest that the purified COP9 complex contains 12 distinct subunits, including COP9 and COP11, and each subunit is present in a 1:1 molar ratio. The predicted total molecular mass of the COP9 complex is 550 kDa, very close to the 560 kDa molecular mass revealed by the gel filtration analysis of the complex.

COP1 Nuclear Translocation in the Dark Depends on the COP9 Complex

Based on the β-glucuronidase–*COP1* (*GUS–COP1*) fusion gene studies, it was proposed that COP1 acts inside the nucleus to suppress photomorphogenic development in darkness, while light inactivation resulted in a nuclear exclusion of COP1 (von Arnim and Deng, 1994). To test whether the COP9 complex plays a role in the light-regulated subcellular localization of COP1, we introduced the biologically active *GUS–COP1* translational fusion transgene into the *cop9* mutant background by standard genetic crosses and examined its subcellular localization by GUS activity staining. In *cop9* mutants grown in darkness, GUS–COP1 fails to enrich in the nuclei of hypocotyl cells (Figure 2). This suggests that COP9 is required for proper COP1 nuclear localization in the dark. As a GUS–NIa fusion protein (Carrington et al., 1991) properly localizes to the nucleus in both dark- and light-grown *cop9* plants, the effect of the *cop9* mutation on GUS–COP1 localization is specific and not an artifact of defective general nuclear transport (Figure 2). Similar results were also obtained for the subcellular localization of GUS–COP1 in *cop8* and *cop11* mutants (data not shown), both of which fail to accumulate the COP9 complex. Therefore, we conclude that the COP9 complex plays a specific role in either the nuclear localization or nuclear retention of COP1 in darkness. This functional interaction would be consistent with the similar pleiotropic photomorphogenic phenotypes in the *cop1*, *cop9*, and *cop11* mutants.

The COP9 Complex Is Nuclear Localized

As a necessary step to understand the cellular basis of COP9 complex function and its role in regulating COP1 nuclear abundance, we examined the subcellular localization of COP9. As all detectable COP9 is present in the complexed form, the subcellular localization pattern of COP9 is expected to be identical to that of the COP9 complex. Indirect immunofluorescence staining (Matsui et al., 1995) of COP9 in protoplasts isolated from cauliflower seedlings (Figure 3A, red) indicated a nuclear localization, which overlaps with nucleus DNA staining of 4′,6-diamidino-2-phenylindole (DAPI) (Figure 3B), while the staining signal derived from the anti-tubulin antibody (Figure 3A, green) exhibited the expected cytoplasmic localization, which was excluded from both the nucleus and vacuole.

To substantiate this observation, a *GUS–COP9* translational gene fusion, under the control of the cauliflower mosaic virus 35S promoter, was introduced into Arabidopsis through Agrobacterium-mediated stable transformation. The subcellular localization of the GUS–COP9 fusion protein was examined by GUS activity staining of both light- and dark-grown seedlings. Consistent with the protoplast immunofluorescence staining pattern of endogenous COP9 in cauliflower, nuclear localization of GUS–COP9 in the young root cells was observed in both light- and dark-grown seedlings (Figures 3C and 3D). This GUS staining pattern is very similar to that of the known nuclear localized GUS–NIa fusion protein (Figure 3F; Carrington et al., 1991; von Arnim and Deng, 1994). While GUS itself is clearly cytoplasmic in transgenic plants, as expected, it was evident that COP9 was able to bring an otherwise cytoplasmic localized GUS protein into the nucleus as a GUS–COP9 fusion protein.

The Nuclear Localization of GUS–COP9 Depends on Functional COP8 and COP11

While GUS–COP9 was translocated into the nucleus in transgenic Arabidopsis (Figure 3), the COP9 sequences do not contain any conserved nuclear translocation signal. This raises the possibility that GUS–COP9 nuclear translocation may require either some degree of the COP9 complex assembly or the function of other pleiotropic *COP/DET/FUS* genes. To test this, we introduced the *GUS–COP9* fusion transgene into six pleiotropic *cop/det* mutant backgrounds by genetic crosses and analyzed the cellular GUS activity staining patterns of young root cells (Figure 4). In *cop1*, *det1*, *cop9*, and

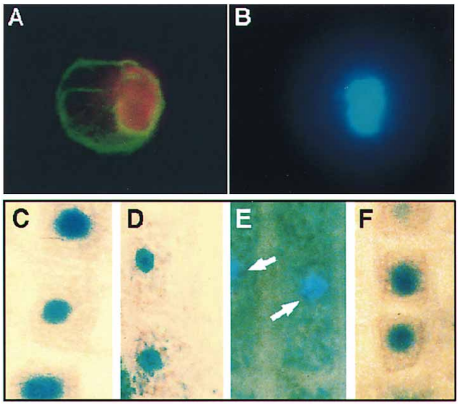

Figure 3. COP9 Is Localized to the Nucleus

(A and B) COP9 subcellular localization in isolated cauliflower seedling protoplasts. The same cell was double stained (A) with affinity-purified anti-cop9 antibodies (red stain) and anti-tubulin monoclonal antibodies (green) and stained with DAPI (B) to show the position of the nucleus.

(C–F) Cellular staining patterns of GUS–COP9, GUS–NIa, and GUS proteins in the root cells of transgenic wild-type Arabidopsis seedlings. (C) and (D) show light-grown and dark-grown *GUS–COP9* transgenic plants, respectively. For cytoplasmic staining of GUS alone (E), the bright field was superimposed on the DAPI labeling to show the position of the nuclei (indicated by arrows). In (F), nuclear staining of GUS–NIa is shown.

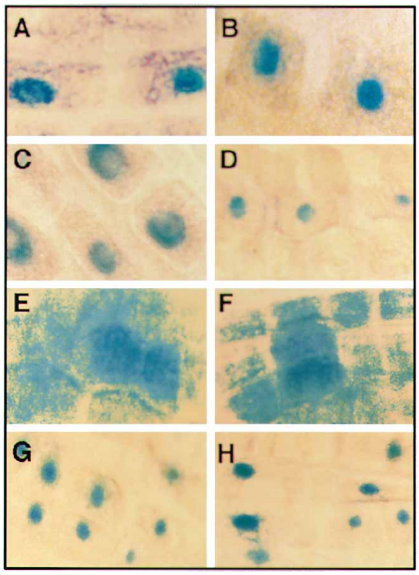

Figure 4. The GUS–COP9 Subcellular Staining Patterns in Young Root Cells of Pleiotropic *cop/det* Photomorphogenic Mutant Seedlings

The *GUS–COP9* transgene from the wild type (see Figure 3) was introduced into *cop1-4* (A), *det1-1* (B), *cop9-1* (C), *cop10-1* (D), *cop8-1* (E), and *cop11-1* (F) mutants by genetic crosses. The control transgene, *GUS–NIa*, was introduced into *cop8-1* and *cop11-1* mutants and results in an identical nuclear localization pattern as in wild type. The GUS staining patterns of GUS–NIa in *cop8-1* (G) and *cop11-1* (H) are shown. Both dark- and light-grown mutant seedlings exhibited identical subcellular GUS staining patterns, and only the results from the light-grown seedlings are shown.

cop10 mutants, GUS–COP9 exhibited a nuclear staining pattern identical to that of wild type (Figures 4A–4D). In *cop8* and *cop11*, however, the GUS–COP9 staining pattern was cytoplasmic (Figures 4E and 4F), indicating that GUS–COP9 can no longer localize to the nucleus in these strains. Since GUS–NIa was able to localize to the nuclei in root cells of both *cop8* and *cop11* mutants (Figures 4G and 4H), it is clear that these mutants are not defective in general nuclear translocation. Therefore, the effects of *cop8* and *cop11* mutations are specific for GUS–COP9. Since COP11, and probably COP8, are components of the COP9 complex, the above result indicates that some degree of preassembly of the COP9 complex is essential for its nuclear translocation.

Discussion

We report here the purification and initial characterization of the nuclear localized COP9 complex. The purified COP9 complex, which is comprised of 12 distinct subunits, is sufficient for peptide sequence analysis of the individual components and thus should permit the cloning and characterization of all subunits of the complex. While previous genetic analysis of the pleiotropic *COP/DET/FUS* loci suggested that they play important roles in the light control of a developmental switch and act downstream of multiple photoreceptors, their functional relationships were largely unknown. Our data show directly that at least two of the pleiotropic *COP/DET/FUS* loci encode components of the same complex, convincingly confirming a genetic prediction that at least some of the pleiotropic *COP/DET/FUS* gene products act as a multiprotein complex.

Mutations in ten available pleiotropic *COP/DET/FUS* loci give essentially identical photomorphogenic phenotypes in the dark (Miséra et al., 1994; Kwok et al., 1996), suggesting that these gene products may act in the same regulatory pathway. The present work has shown that, while some of the proteins (COP9 and COP11) encode subunits of the same regulatory complex, others (such as COP1 and DET1) are not components of the purified complex (data not shown). This raises the next question: what are the relationships between the COP9 complex and the other pleiotropic *COP/DET/FUS* gene products that are not part of the complex?

We have shown previously that the COP9 complex is larger in the dark than in the light, where it is around 560 kDa (Wei et al., 1994b). The "dark" form is extremely unstable and can be completely converted to the stable "light" form within a couple of minutes after exposure to even dim light. The size of the purified COP9 complex correlates with that of the light complex form. While COP1 and DET1 do not appear to be components of the light COP9 complex (data not shown), it is possible that they are either components of the dark complex or interact transiently with the complex. Since both COP1 and DET1 are located in the nucleus in the dark, these interactions are physically feasible. In the case of COP1, this interaction may happen only in the dark, since COP1 is presumably depleted in the nucleus under light conditions.

Supporting evidence for a functional interaction between COP1 and the COP9 complex is found in the

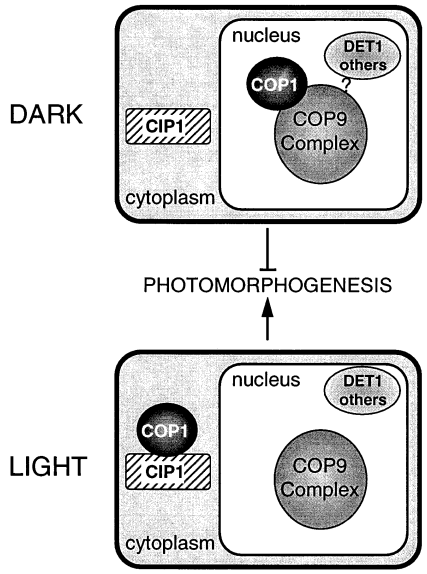

Figure 5. Model for the Cellular Action of the COP9 Complex

In the dark, the COP9 complex interacts with COP1 and possibly DET1 in repressing photomorphogenesis. Light causes the dissociation of COP1 from the complex and its repartition to the cytoplasm, where it binds CIP1 (Matsui et al., 1995), allowing photomorphogenesis to proceed.

nonreciprocal dependence of COP1 on COP9 for nuclear localization. COP1 has a direct role in light signaling, as its subcellular localization is both light and tissue dependent (von Arnim and Deng, 1994) and its overexpression leads to partial repression of photomorphogenic development even under light conditions (McNellis et al., 1994b). Since the COP9 complex is larger in dark-grown Arabidopsis seedlings and the nuclear localization of COP1 in the dark is disrupted in *cop9* mutants, one appealing model would have COP1 interacting with the COP9 complex in the dark to repress photomorphogenesis, while light causes the dissociation of COP1 from the complex and the export or degradation of nuclear COP1, leaving the smaller "light" COP9 complex (Figure 5). However, COP1 does not appear to interact directly with either COP9 or COP11, as several direct interaction assays led to negative results (data not shown). Therefore, the hypothesized interaction between COP1 and the COP9 complex is likely to be mediated through another component(s), indirectly through an intermediate component(s), or require specific protein modifications.

Our data indicated that the COP9 complex is a multisubunit nuclear regulator and has the potential for directly interacting with nucleic acids. The high similarity of both COP9 and COP11 to their human counterparts over the entire length of the proteins implies that they may represent homologous proteins between Arabidopsis and humans (Chamovitz and Deng, 1995), suggesting that the COP9 complex may represent a novel yet conserved development regulator in both animal and plant kingdoms. It is worth mentioning that the human COP11-like protein has been cloned as a high copy repressor of the yeast *gpa1* mutant (K. S. Bowdish and J. Colicelli, personal communication; GenBank accession number U20285), which is defective in the α subunit of the trimeric G protein involved in the pheromone response pathway (Dietzel and Kurjan, 1987). This raises the possibility that COP11 has the potential for interacting with a heterotrimeric G protein–potentiated signaling pathway. This would be consistent with the observation that a trimeric G protein(s) was involved in the photoreceptor phytochrome signaling (Bowler and Chua, 1994). Clearly, elucidating the molecular mechanism of the COP9 complex action will provide important insights into light control of a developmental switch.

Experimental Procedures

Purification of the COP9 Complex

All steps were carried out at 4°C. Cauliflower (Brassica oleracea var. Botrytis) heads were purchased from local markets. Apical tissue from cauliflower heads (approximately the top 3–7 mm surface layer), comprised primarily of floral and inflorescence meristems, was collected and passed twice through a Champion juicer (Plasta-ket Manufacturing Co.) with constant addition of extraction buffer (200 mM NaCl and 0.5 mM PMSF at 100 ml per 100 g in buffer A, which contains the following: 50 mM $NaHPO_4$ [pH 7.0], 10 mM $MgCl_2$, 5 mM β-mercaptoethanol, 10% glycerol). After filtration through four layers of cheesecloth and four layers of Miracloth (Calbiochem), insoluble cell debris was pelleted at 13,000 $\times$ g for 90 min. The supernatant was carefully poured over a 10 cm long 2.5 cm diameter glass wool–filled column, and the flowthrough was collected. This was applied to a 600 ml Q Sepharose Fast Flow column (Pharmacia), equilibrated in buffer A with 200 mM NaCl. Following a wash in buffer A with 200 mM NaCl, COP9 was eluted in 500 mM NaCl in buffer A. The eluate was diluted with equal volume buffer B (20 mM bis-Tris propane [pH 7.0], 10 mM $MgCl_2$, 0.5 mM PMSF, 5 mM β-mercaptoethanol, 10% glycerol) and buffer exchanged to buffer B, and the sample was concentrated to 150 ml by diafiltration over a 300 kDa Ultrasette (Filtron). The retentate from the diafiltration was cleared by centrifugation at 45,000 $\times$ g and applied to a 60 ml Q Sepharose HP column (Pharmacia) equilibrated in buffer B. COP9 was eluted in a linear gradient of 0–500 mM NaCl in buffer B. COP9-containing fractions were pooled, diluted with equal volume buffer B, and applied to a 5 ml HiTrap heparin column (Pharmacia) equilibrated in buffer B. The complex was eluted with 600 mM NaCl in buffer B. The heparin eluate was diluted 1$\times$ in buffer C (20 mM bis-Tris [pH 5.7], 10 mM $MgCl_2$, 10% glycerol) and diafiltered twice on a 100 kDa Macrosep (Filtron). The retentate was applied to a Mono Q HR5/5 column (Pharmacia) equilibrated in buffer C, and COP9 was eluted as the major peak in a linear gradient of 130–350 mM NaCl in buffer C. The COP9-containing fractions were pooled and concentrated to 100 μl on a 100 kDa Microsep (Filtron) and applied to Superose 6 HR10/30 column (Pharmacia) equilibrated in buffer D (50 mM $NaHPO_4$ [pH 7.4], 10 mM $MgCl_2$, 150 mM NaCl, 10% glycerol). The COP9 complex was collected as a single peak eluting at 560 kDa.

Protein Analysis and Peptide Sequencing

The purified COP9 complex was separated on a 10%–12.5% polyacrylamide gel and stained for 30 min in 50% methanol, 10% acetic acid, 0.1% Coomassie blue. Following destaining in 50% methanol, 10% acetic acid for 3 hr, individual protein bands were excised with a razor blade. Prior to proteolytic digestion, 10% of several of the excised bands was hydrolyzed, the amino acids were separated on a Beckman 7300 HPLC, and the total protein content was estimated. The gel slices were digested in gel with either Achromobacter protease I or trypsin. After complete enzymatic digestion, peptides were separated by reverse-phase HPLC, and thus a profile could be obtained. Individual peptides were analyzed for purity and amount by matrix-assisted laser desorption mass spectrometry (MALDI-TOF) (Bruker). The peptides chosen were sequenced on an ABI 477A peptide-sequencing instrument. From the peptide amount and its exact amino acid sequence, its molar amount was calculated.

Electron Microscopy

The purified complex from peak II was negatively stained on a glow-discharged Formvar grid with 3% (w/v) uranyl acetate. The negatively stained sample was examined by electron microscopy in a Zeiss EM-10 electron microscope at a magnification of 160,000×.

Protoplast Immunofluorescence Staining and Protein Analysis

Protoplasts were prepared according to Matsui et al. (1995). The primary antibodies used in this work were as follows: affinity-purified rabbit polyclonal antibodies against COP9 at 1:200; monoclonal anti-α-tubulin antibody from mouse ascites fluid (clone DM 1A; Sigma) at 1:400; and Y12. Secondary antibodies were fluorescein-conjugated anti-mouse (Molecular Probes) or Cy3-conjugated anti-rabbit (Sigma).

Plant tissue homogenization, analytic gel filtration analysis, and immunoblot analysis of total protein extract were according to Wei et al. (1994b). The COP11 antibodies were raised against the E. coli–expressed Arabidopsis COP11 and affinity purified (J. M. S. and X.-W. D., unpublished data).

Analysis of GUS Subcellular Localization in Arabidopsis Seedlings

The *GUS–COP9* fusion gene was constructed by ligating a 0.7 kb BamHI fragment containing the entire *COP9* cDNA to a BglII–BamHI-cut pRTL-2-GUS-NIaΔBam plasmid. Transgenic plants were generated and analyzed as described previously for GUS–COP1 (von Arnim and Deng, 1994).

Plant Materials and Growth Conditions

The *cop9-1*, *cop8-1*, *cop10-1*, and *cop11-1* mutants are in Wassilewskija background (Wei et al., 1994a), while *cop1-4* and *det1-1* are in COL-O ecotype (McNellis et al., 1994a; Pepper et al., 1994). Unless otherwise specified, all transgenic and wild-type plants are in No-O ecotype. Plant germination and growth conditions in darkness and white light were as described previously (McNellis et al., 1994a). Light/dark cycle conditions of 16 hr of white light at 75 mmol m^{-2} s^{-1} and 8 hr of darkness was used for light-grown seedlings.

Acknowledgments

Correspondence should be addressed to X.-W. D. We thank Drs. Naoshi Dohmae and Koji Takio of the Division of Biomolecular Characterization (RIKEN, Japan) for assistance in protein digestion and peptide sequencing; the W. M. Keck Foundation Biotechnology Resource Laboratory at Yale University for amino acid analysis; Prof. Ethan Signer for advising in large-scale tissue homogenization; Barry Piekos for assistance with electron microscopy; and Prof. Arthur Galston for critical reading of the manuscript. This research was supported by a National Science Foundation (NSF) grant (MCB-9513366) to X.-W. D. X.-W. D. is an NSF Presidential Faculty Fellow, D. A. C. is a postdoctoral fellow of the International Human Frontier Science Program, M. T. O. is a National Institutes of Health (NIH) predoctoral trainee, and J. M. S. is a NIH postdoctoral fellow.

Received March 22, 1996; revised May 15, 1996.

References

Ahmad, M., and Cashmore, A.R. (1993). HY4 gene of *A. thaliana* encodes a protein with characteristics of a blue-light photoreceptor. Nature *366*, 162–166.

Bowler, C., and Chua, N.H. (1994). Emerging themes of plant signal transduction. Plant Cell *6*, 1529–1541.

Carrington, J.C., Freed, D.D., and Leinicke, A.J. (1991). Bipartite signal sequence mediates nuclear translocation of the plant potyviral NIa protein. Plant Cell *3*, 953–962.

Castle, L., and Meinke, D. (1994). A *FUSCA* gene of *Arabidopsis* encodes a novel protein essential for plant development. Plant Cell *6*, 25–41.

Chamovitz, D.A., and Deng, X.-W. (1995). The novel components of the Arabidopsis light signaling pathway may define a group of general developmental regulators shared by both animal and plant kingdoms. Cell *82*, 353–354.

Deng, X.-W., Matsui, M., Wei, N., Wagner, D., Chu, A.M., Feldmann, K.A., and Quail, P.H. (1992). *COP1*, an Arabidopsis regulatory gene, encodes a protein with both a zinc-binding motif and a G_β homologous domain. Cell *71*, 791–801.

Dietzel, C., and Kurjan, J. (1987). The yeast SCG1 gene: a G-like protein implicated in the a- and α-factor response pathway. Cell *50*, 1001–1010.

Kwok, S.F., Piekos, B., Miséra, S., and Deng, X.-W. (1996). A complement of ten essential and pleiotropic *Arabidopsis COP/DET/FUS* genes are necessary for repression of photomorphogenesis in darkness. Plant Physiol. *110*, 731–742.

Matsui, M., Stoop, C.D., von Arnim, A.G., Wei, N., and Deng, X.-W. (1995). *Arabidopsis* COP1 protein specifically interacts *in vitro* with a cytoskeleton-associated protein, CIP1. Proc. Natl. Acad. Sci. USA *92*, 4239–4243.

McNellis, T.W., and Deng, X.-W. (1995). Light control of seedling morphogenetic pattern. Plant Cell *7*, 1749–1761.

McNellis, T.W., von Arnim, A.G., Araki, T., Komeda, Y., Miséra, S., and Deng, X.-W. (1994a). Genetic and molecular analysis of an allelic series of cop1 mutants suggests functional roles for the multiple protein domains. Plant Cell *6*, 487–500.

McNellis, T.W., von Arnim, A.G., and Deng, X.-W. (1994b). Overexpression of *Arabidopsis COP1* results in partial suppression of light-mediated development: evidence for a light-inactivable repressor of photomorphogenesis. Plant Cell *6*, 1391–1400.

Miséra, S., Muller, A.J., Weiland-Heidecker, U., and Jurgens, G. (1994). The *FUSCA* genes of *Arabidopsis*: negative regulators of light responses. Mol. Gen. Genet. *244*, 242–252.

Pepper, A., Delaney, T., Washburn, T., Poole, D., and Chory, J. (1994). *DET1*, a negative regulator of light-mediated development and gene expression in Arabidopsis, encodes a novel nuclear-localized protein. Cell *78*, 109–116.

Quail, P.H., Boylan, M.T., Parks, B.M., Short, T.W., Xu, Y., and Wagner, D. (1995). Phytochromes: photosensory perception and signal transduction. Science *268*, 675–680.

von Arnim, A.G., and Deng, X.-W. (1994). Light inactivation of Arabidopsis photomorphogenic repressor COP1 involves a cell-specific regulation of its nucleocytoplasmic partitioning. Cell *79*, 1035–1045.

Wei, N., Kwok, S.F., von Arnim, A.G., Lee, A., McNellis, T.W., Piekos, B., and Deng, X.-W. (1994a). *Arabidopsis COP8*, *COP10*, and *COP11* genes are involved in repression of photomorphogenic development in darkness. Plant Cell *6*, 629–643.

Wei, N., Chamovitz, D.A., and Deng, X.-W. (1994b). Arabidopsis COP9 is a component of a novel signaling complex mediating light control of development. Cell *78*, 117–124.